Chem. Mater. **2001,** *13,* 1665−1673

Steric Control of Conductivity in Highly Conjugated Polythiophenes

T. Benincori,[‡] V. Consonni,[§] P. Gramatica,[||] T. Pilati,[#] S. Rizzo,[†] F. Sannicolò,*,[†]
R. Todeschini,[§] and G. Zotti[⊥]

Dipartimento di Chimica Organica e Industriale dell'Università di Milano e Centro CNR Sintesi e Stereochimica Speciali Sistemi Organici, via C.Golgi 19, 20133 Milano, Italy, Dipartimento di Scienze Chimiche, Fisiche e Matematiche dell'Università dell'Insubria, via Lucini 3, 22100 Como, Italy, Dipartimento di Scienze dell'Ambiente e del Territorio dell'Università di Milano-Bicocca, P.za della Scienza 1, 20126 Milano, Italy, Dipartimento di Biologia Strutturale e Funzionale dell'Università dell'Insubria, Via J. H. Dunant 2, 21100 Varese, Italy, Istituto di Polarografia ed Elettrochimica Preparativa, Consiglio Nazionale delle Ricerche, c.so Stati Uniti 4, 35020 Padova, Italy, and Centro CNR per lo Studio delle Relazioni fra Struttura e Reattività Chimica, via C.Golgi 19, 20133 Milano, Italy

Received November 16, 2000. Revised Manuscript Received February 14, 2001

A series of 4-alkylidene-, 4-alkyl-, and 4,4′-dialkyl-substituted 4H-[5,1-b;1,5-b′]cyclopentabithiophenes was designed in which the substituents in position 4 occupy well-defined areas in the space around the bithiophene unit to evaluate the effects played by their steric properties on the electrical conductivity of the materials resulting from anodic polymerization. The geometry of all the monomers was either inferred from X-ray diffractometric analysis or calculated through molecular modeling techniques. The polymers were prepared under identical experimental conditions and characterized by CV, IR, and UV−vis spectroscopy and in situ conductivity. Various types of molecular descriptors were utilized to create QSPR models, which demonstrated a good relationship between the molecular structure of the monomers and the conductivity of the corresponding polymers.

Introduction

The modern design of functionalized electroconductive polymers is based on the construction of models in which specific structural parameters may be controlled to verify their effects on the properties of the material.[1] One of the most significant properties of these materials is specific conductivity, even though, in the field of organic semiconductors, many other physical features are relevant.

The main parameters that are known to directly influence conductivity of electrochemically prepared conjugated materials and of five-membered poly-heteroaromatic systems in particular are as follows:

(1) The electronic availability of the monomer heterocyclic unit.

It is well-known that the presence of electron-releasing substituents on the starting polymerogenic unit facilitates anodic coupling, thus making it possible to obtain polymeric materials featuring high conductivity and a low optical energy gap.[2] For instance, the introduction of one or two alkoxy groups in the β positions of a thiophene ring improves both the electronic and optical properties of polythiophene.[3] This effect has been attributed to a statistical reduction of constitutional defects related to $\alpha-\beta$ and $\beta-\beta$ junctions.

(2) The length of the π conjugation in the single polymeric chain.[4]

Experimental measurements of the macroscopic conductivity of polythiophene-based materials and theoretical calculations have shown that long sequences of conjugated heteroaromatic rings are necessary to achieve optimal conductivity in the doped state.[5] Current transport in polymeric materials takes place through thermally activated hopping of bipolaron charge carriers, injected into the single macromolecule upon oxidative doping. It is believed that the electronic delocalization along the polymeric chain favors mobility through intrachain hopping.

(3) The supramolecular organization of polymeric chains.

[†] Università di Milano.

[‡] Dipartimento di Scienze Chimiche, Fisiche e Matematiche dell'Università dell'Insubria.

[§] Università di Milano-Bicocca.

[||] Dipartimento di Biologia Strutturale e Funzionale dell'Università dell'Insubria.

[⊥] Consiglio Nazionale delle Ricerche.

[#] Centro CNR per lo Studio delle Relazioni fra Struttura e Reattività Chimica.

(1) McQuade, D. T.; Pullen, A. E.; Swager, T. M. *Chem. Rev.* **2000**, *100*, 2537.

(2) Elsenbaumer, R. L.; Jen, K.-Y.; Miller, G. G.; Eckhardt, H.; Shacklette, L. W.; Jow, R. In *Electronic Properties of Conjugated Polymers*; Springer Series in Solid State Sciences 76; Springer: Berlin, 1987; p 400.

(3) Tanaka, S.; Sato, M. A.; Kaeriyama, K. *Synth. Met.* **1988**, *25*, 277. Feldhues, M.; Kampf, G.; Litterer, H.; Mechlenburg, T.; Wegener, P. *Synth. Met.* **1989**, *28*, C487. Yamamoto, T.; Kashiwazaki, A.; Kato, K. *Makromol. Chem.* **1989**, *190*, 1649. Roncali, J.; Marque, P.; Garreau, R.; Garnier, F.; Lemaire, M. *Macromolecules* **1990**, *23*, 1347. Daoust, G.; Leclerc, M. *Macromolecules* **1991**, *24*, 455.

(4) McCullough, R. D. *Adv. Mater.* **1998**, *10*, 93.

(5) Baughman, R. H.; Shacklette, L. W. *Phys. Rev. B* **1989**, *39*, 5872; Roth, S.; Bieier, H.; Pukacki, W. *Faraday Discuss. Chem. Soc.* **1989**, *88*, 223, and references therein.

10.1021/cm0009118 CCC: $20.00

It was found that the degree of packing influences the interchain contribution to electrical conductivity. Investigations on this point demonstrated the crucial influence of counterion size and of bulkiness of the substituents on the morphological properties of a polymer.[6] For example, it was suggested that the occurrence of interchain charge hopping in poly(3,4-cycloalkylthiophenes)[7] and poly(3,4-cycloalkylpyrroles)[8] might be controlled by ring dimension because the conductivity log was found linearly dependent upon the ring diameter, as evaluated by X-ray diffractometric analysis of the starting monomers.

The aim of the present research is to contribute to the knowledge of the geometrical and steric parameters describing the structure of the monomers that control the supramolecular organization of the chains of the corresponding polymers in bithiophene-based materials and to quantitatively investigate their effects on conductivity.

This project is aligned with a recent development in sensor research regarding volatile organic compound (VOC) detection based on polymer array devices exploiting conductivity changes upon solvent swelling.[9] Polythiophene-based systems, characterized by substituents featuring different shapes and sizes, represent a challenging alternative to polypyrrole-based sensors, differing in counteranion stereoelectronic properties.[10]

The research was developed according to the following guidelines:

(1) Design of bithiophene-based monomers functionalized with substituents endowed with well-defined architectures, extending into specific space regions.

(2) Synthesis and chemical characterization of the monomers.

(3) Study of the geometry of all the monomers by X-ray diffractometric analysis and molecular modeling calculations.

(4) Anodic polymerization of all the monomers under identical experimental conditions and spectroscopic and electrochemical characterization of the resulting materials.

(5) Search for possible quantitative relationships (QSPR approach) between the geometric parameters describing the morphology of the monomers and the electrical properties of the resulting polymers.

If successful, the results of this research could be very helpful for designing and structurally optimizing new monomers capable of producing materials possessing high electrical conductivity.

Results and Discussion

(1) Design of Monomers. The structural design of the monomers was realized according to the following guidelines:

(i) At the level of choice of a bithiophene polymerogenic unit and the substituents, the design of the monomers had to be developed in such a way as to preserve a substantially constant electronic intrachain situation in all the resulting polymers.

(ii) Substituents on the thiophene ring should possess the following structural characteristics: (a) first of all, they should display well-defined geometrical properties and consequently possess a certain degree of structural rigidity; (b) because steric effects need to be much more relevant than electronic effects, the design of the substituents calls for electronically neutral groups, unable to exert consistent perturbation of the electronic situation present in the unsubstituted polybithiophene backbone.

(iii) Monomer design should guarantee, at least in principle, the homotopism of the positions that are involved in the polymerization process. Constitutionally, heterotopic polymerization sites produce constitutionally different, noncomparable materials, while coupling of enantiotopic centers causes some stereochemical disorder in the polymer.

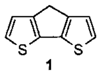

1

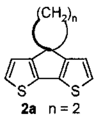

2a n = 2
2b n = 3
2c n = 4
2d n = 5

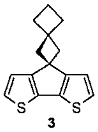

3

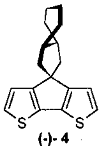

(-)- 4

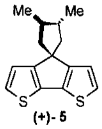

(+)- 5

In light of these requirements, we chose as the basic polymerogenic unit 4H-cyclopenta[2,1-b;3,4-b′]dithiophene (CPDT) (**1**), a bithiophene unit designed by us some years ago and made accessible through a convenient four-step synthesis.[11] The reasons for this choice are as follows: (a) unsubstituted CPDT (C_{2v} symmetry) shows homotopic α and α′ positions; (b) CPDT is known to give polymers possessing extended π conjugation and good conductivity; (c) functionalization of CPDT in position 4 is easy, taking advantage of the acidic hydrogen atoms present on it; (d) the presence of substituents, even bulky,[12] in position 4 of CPDT allows the evaluation of the effects on polymer properties of the volume and shape of the substituents free of the effects produced by interanular torsion which, as a rule, occurs in 3,4-disubstituted polythiophenes. This kind of distortion is expected, for instance, in the case of the above-mentioned poly(3,4-cycloalkyl)thiophenes.[7]

According to the outlined guidelines, two classes of 4-substituted CPDTs were designed. The first one carries cyclic rings directly bonded to sp^3-hybridized spiranic C$_4$ of CPDT. The ring should be predominantly arranged on a plane perpendicular to that of the CPDT unit.

---

[6] McCullough, R. D.; Tristram-Nagle, S.; Williams, S. P.; Lowe, R. D.; Jayaraman, M. *J. Am. Chem. Soc.* **1993**, *115*, 4910. McCullough, R. D.; Williams, S. P.; Tristram-Nagle, S.; Jayaraman, M.; Ewbank, P. C.; Miller, L. *Synth. Met.* **1995**, *69*, 279.

[7] Ruhe, J.; Berlin, A.; Wegner, G. *Macromol. Chem. Phys.* **1995**, *196*, 225.

[8] Ruhe, J.; Krohnke, C.; Ezquerra, T.; Kremer, F.; Wegner, G. *Ber. Bunsen-Ges. Phys. Chem.* **1987**, *91*, 885. Ruhe, J.; Ezquerra, T.; Mohammadi, M.; Enkelmann, V.; Kremer, F.; Wegner, G. *Synth. Met.* **1989**, *28*, C217.

[9] Eastman, M. P.; Hughes, R. C.; Yelton, G.; Ricco, A. J.; Patel, S. V.; Jenkins, M. W. *J. Electrochem. Soc.* **1999**, *146*, 3907. Patel, S. V.; Jenkins, M. W.; Hughes, R. C.; Yelton, W. G.; Ricco, A. J. *Anal. Chem.* **2000**, *72*, 1532. Lonergan, M. C.; Severin, E. J.; Doleman, B. J.; Beaber, S. A.; Grubbs, R. H.; Lewis, N. S. *Chem. Mater.* **1996**, *8*, 2298. Severin, E. J.; Lewis, N. S. *Anal. Chem.* **2000**, *72*, 2008.

[10] deSouza, J. E. G.; Neto, B. B.; dos Santos, F. L.; deMelo, C. P.; Santos, M. S.; Ludemir, T. B. *Synth. Met.* **1999**, *102*, 1296.

[11] Benincori, T.; Brenna, E.; Sannicolò, F.; Trimarco, L.; Moro, G.; Pitea, D.; Pilati, T.; Zerbi G., Zotti G. *J. Chem. Soc. Chem. Commun.* **1995**, 881.

[12] Benincori, T.; Brenna, E.; Sannicolò, F.; Trimarco, L.; Zotti, G.; Sozzani, P. *Angew. Chem., Int. Ed. Engl.* **1996**, *35*, 648.

Substrates **2a**−**d** and **3**−**5** belong to this class. In substrates **3**−**5** there is a further out-of-plane extension of the cycloalkyl system in areas more distant from the core of the polymerogenic unit.

All the substituents retain the C_2 symmetry molecular axis present in CPDT and thus the homotopism of the α and α′ positions. Furthermore, because **4** and **5** are C_2 symmetry chiral compounds, we considered it important to make use of pure enantiomers because stereochemical disorder is unavoidable in materials resulting from racemates.

The second class of monomers results from functionalization at C_4 of CPDT with a double bond. This strategy allows placement of substituents predominantly on the plane of the CPDT scaffold. Substrates **6**−**7** belong to this class. In substrates **8** and **9** suitably branched substituents to the hexocyclic double bond make it possible to occupy specific portions of the half-spaces above and below the CPDT plane.

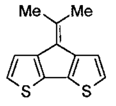
6

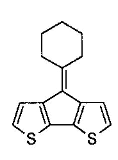
7

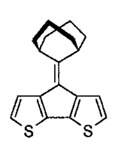
8

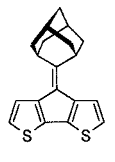
9

The substantial rigidity of the substituents, which is the common structural characteristic of the members of these two classes, permits rather simple analysis of their geometries and, above all, guarantees that they occupy very well-defined areas in the space.

Some other already known monomers have been considered when their synthesis and the characterization of the materials derived from their electrochemical polymerization were described with satisfactory experimental documentation. Selection of these systems was conditioned by several basic requirements: anodic oxidation was carried out under the same experimental conditions we had chosen for our substrates and electrical conductivity of the polymers was evaluated in situ, according to the same procedure we employed for the materials prepared by us. Compounds **10a**−**10c**[13] and **11**[13] fit well in the series of 4-alkylidene derivatives. Their drawback, at first glance, is a possible influence of the electronic effects of the substituent on the cyclopentabithiophene system.

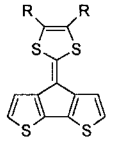

10

a: R = H
b: R = Me
c: R = SMe

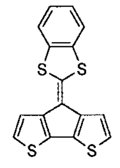
11

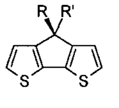

12

a: R = H, R′ = Me
b: R = H, R′ = $(CH_2)_2Me$
c: R = H, R′ = $(CH_2)_3Me$
d: R = H, R′ = $(CH_2)_5Me$
e: R = H, R′ = $(CH_2)_7Me$
f : R = R′ = Me
g: R = R′ = $(CH_2)_2Me$
h: R = R′ = $(CH_2)_3Me$
i : R = R′ = $(CH_2)_5Me$
l : R = R′ = $(CH_2)_7Me$

Scheme 1

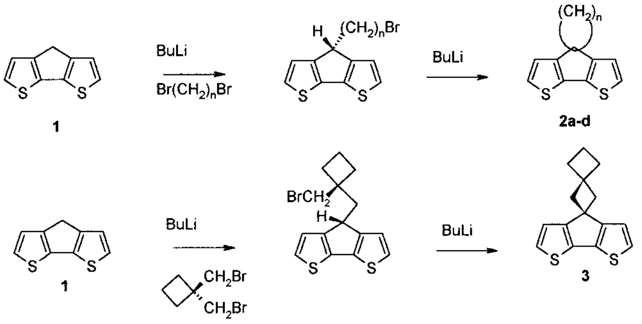

Substrates **12f**−**12l** pertain to the class of 4,4′-disubstituted cyclopentabithiophenes.[14] They are characterized by two identical linear alkyl chains varying in length from C1 to C8. All these compounds possess C_{2v} symmetry and therefore satisfy the requirements for homotopism of the centers involved in the polymerization process. Only short-chain compounds are supplied with a certain degree of rigidity. Those bearing long alkyl chains do not possess well-defined geometries but they were nonetheless included in this study because the favorable effect exerted by linear alkyl chains on the conductivity of polythiophenes is well documented. For the same reason, we also included the five C_s symmetry monomers **12a**−**12e**,[14] which cannot, in theory, provide polymers with a perfectly controlled stereochemical order.

On the whole, we considered 25 monomers and the corresponding polymeric materials, which represent a rather noteworthy number of substrates from which reliable information can be drawn.

(2) Synthesis of the Monomers. Synthesis of spiranic monomers **2a**−**d** and **3** was achieved through double alkylation of the anion of CPDT with a suitable *ω,ω′*-dibromo derivative. All the reactions were performed in two steps, without isolation of the monoalkylated intermediate, as reported in Scheme 1. 1,1′-Bis(bromomethyl)cyclobutane,[15] intermediate for the synthesis of the dispiranic monomer **3**, was prepared starting from 1,3-dibromopropane by reaction with diethylmalonate in the presence of 2 equiv of sodium ethoxyde. The resulting diethyl 1,1′-cyclobutane-dicarboxylate[16] was reduced with $LiAlH_4$ to the corresponding diol,[17] which was converted in turn into the dibromo derivative by reaction of its ditosylate[18] with potassium bromide in DMF solution.

Chiral compounds **(−)-4** and **(+)-5** were prepared by reaction of the anion of CPDT with (+)-(1S,2S)-trans-bis(hydroxymethyl)cyclohexane bis-methanesulfonate **(+)-14** and (−)-(2R,3R)-dimethyl-1,4-butanediol bis-methanesulfonate **(−)-16**, which were prepared by reaction of the corresponding diols **(−)-13**[19] and **(+)-15**[20]

---

[13] Kazaki, M.; Tanaka, S.; Yamashita, Y. *J. Org. Chem.* **1994**, *59*, 442.

[14] Zotti, G.; Schiavon, G.; Berlin, A.; Pagani, G. *Macromolecules* **1994**, *27*, 1938.

[15] Buchta, E.; Merck, W. *Chimia* **1968**, *22*, 193.

[16] Cason, J.; Allen, C. F. *J. Org. Chem.* **1949**, *14*, 6.

[17] Foos, J.; Steel, F.; Rizvi, S. Q. A.; Fraenkel, G. *J. Org. Chem.* **1979**, *44*, 2522.

[18] Schubert, W. M.; Leahy, S. M., Jr. *J. Am. Chem. Soc.* **1957**, *79*, 381.

[19] McCasland, C. E.; Proskow, S. *J. Am. Chem. Soc.* **1956**, *78*, 5646.

[20] Applequist, D. E.; Werner, N. D. *J. Org. Chem.* **1963**, *28*, 48.

Scheme 2

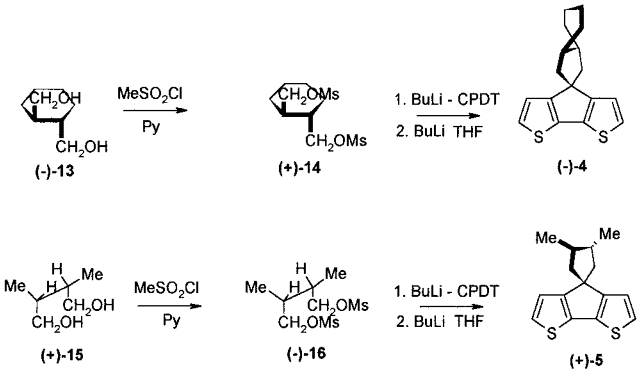

Scheme 3

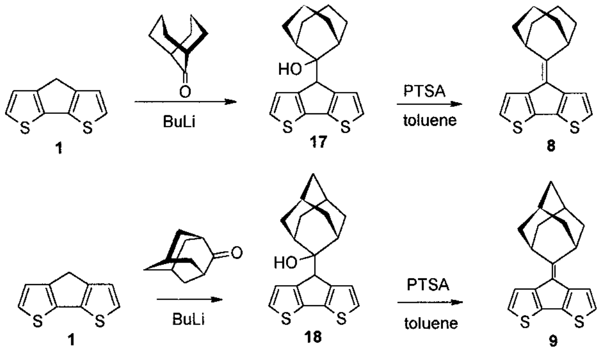

with mesyl chloride in pyridine solution, as reported in Scheme 2.

4-Alkylydene derivatives were prepared by reaction of the anion of **1** with suitable ketones, as reported in Scheme 3. Compounds **6** and **7** were obtained by reaction of the CPDT anion with acetone and cyclohexanone, respectively. The same reaction with bicyclo-[3.3.1]nonan-9-one and 2-adamantanone produced the alcohols **17** and **18**, which were then converted into **8** and **9** by acid-catalyzed dehydration.

All the other monomers were already known in the literature. Only those for which a more accurate characterization was deemed necessary were prepared according to the reported methods.

All new monomers were characterized on the basis of their analytical and spectral properties (see Experimental Section).

(3) Study of the Geometry of All the Monomers. The geometric parameters of new compounds **2d** and **8** were determined by single-crystal X-ray diffractometric analysis (Figures 1 and 2). Crystallographic data were already available for monomers **1**,[21] **2c**,[21] **10a**,[13] and **11**.[13,22]

A comparison was made of the X-ray crystallographic data and computational chemistry geometries to check the reliability of the optimized structures with respect to the crystallographic ones. The minimum energy conformations of all the monomers were obtained by the molecular mechanics method of Allinger (MM+), using the *HYPERCHEM* package.[23]

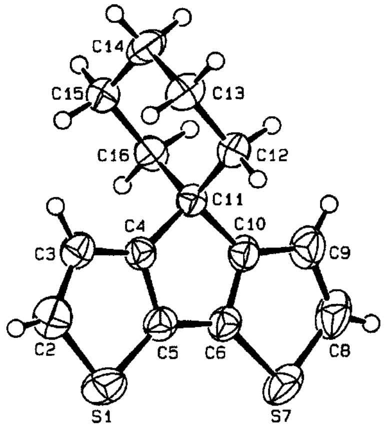

Figure 1. X-ray structure of **2d**.

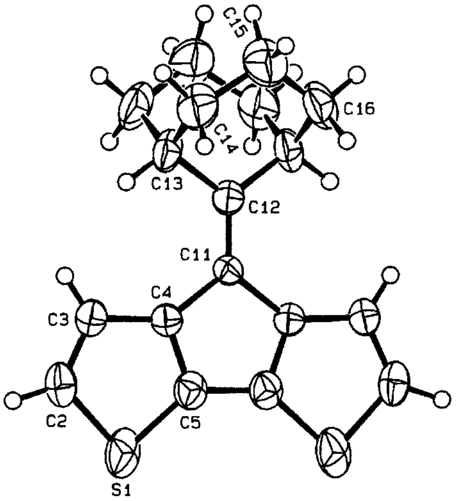

Figure 2. X-ray structure of **8**.

To take into account the three-dimensional (3D) structure of the molecules WHIM (weighted holistic invariant molecular) descriptors[24] were used. The comparison of crystallographic and optimized structures was performed by principal component analysis (PCA) on their WHIM descriptors.

The crystallographic structures (plain symbols) and the corresponding optimized ones (solid symbols), projected on the first two principal component (PC) plane, are shown in Figure 3; the total explained variance is 67.7% (PC1 = 35.6% and PC2 = 32.1%, respectively).

The first two PCs explain the variability due to the different chemical structures of the molecules. While in PC1 a satisfactory agreement between the crystallographic and the calculated structures is observed, a small difference is evident in the second PC2. For all the molecules, this difference is due to carbon−hydrogen bond length, which is always shorter in crystallographic structures than in structures obtained by using molecular mechanics. Moreover, for molecules **10a** and **11** an additional difference can be ascribed to the fact that the crystallographic structures are less conjugated than the corresponding HyperChem calculated structures. Despite some structural differences in these two molecules, a satisfactory agreement was found between crystal-

---

(21) Pilati, T. *Acta Crystallogr.* **1995**, *C51,* 690.

(22) Kozaki, M.; Tanaka, S.; Yamashita, Y. *J. Chem. Soc., Chem. Commun.* **1992**, 1137.

(23) *HYPERCHEM 1995. Rel.4 for Windows*; Autodesk, Inc.: Sausalito, CA, 1995.

(24) Todeschini, R.; Lasagni, M.; Marengo, E. *J. Chemometrics* **1994**, *8,* 263. Todeschini, R.; Gramatica, P. *Quant. Struct.-Act. Relat.* **1997**, *16,* 113.

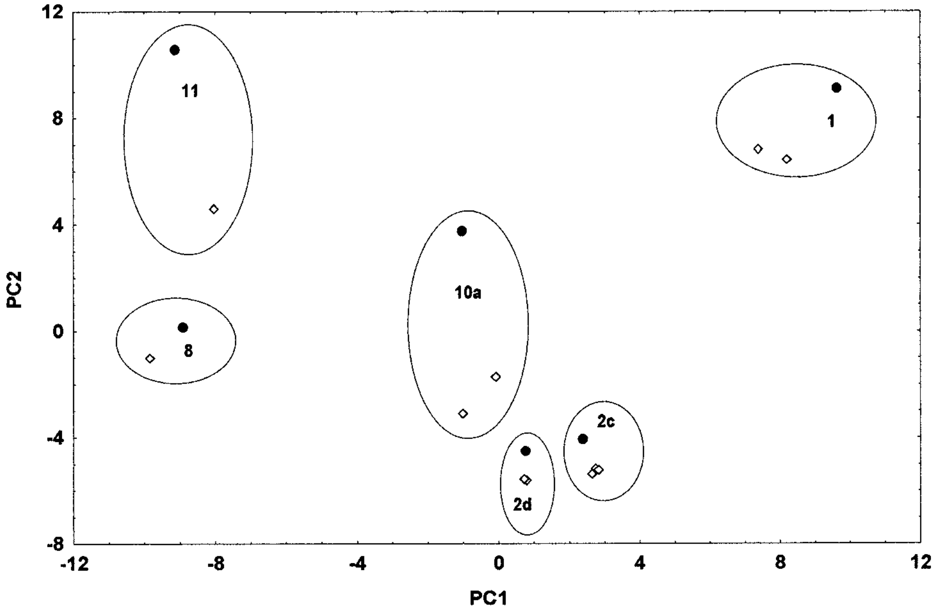

Figure 3. Representation of the crystallographic structures (plain symbols) and the corresponding optimized ones (solid symbols), projected on the first two principal components (PC) plane.

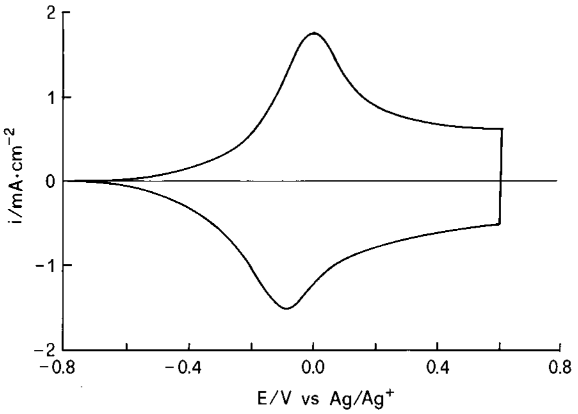

Figure 4. Anodic cyclic voltammogram for poly(**2c**) in $CH_3CN + 0.1$ M Et_4NClO_4. Scan rate: 0.1 V/s. Reversible charge: 8.7 mC/cm^2.

lographic and calculated data. Thus, the homogeneity of the structural information obtained using calculated structures for all the compounds gives a great advantage in modeling procedures.

(4) Electrochemical Polymerization of the Monomers and Electrochemical and Spectroscopic Characterization of the Polymers. Cyclic voltammetry of the monomers was performed in the presence of 0.1 M Et_4NClO_4, in acetonitrile solution. An oxidation peak at 0.6−0.7 V at 0.1 V/s is displayed. Continuous cycling of the potential causes the redox cycle to develop because of the polymer growth on the electrode. Typical cyclic voltammograms of polymer films are shown in Figures 4 and 5.

The ratio of the reversible charge over that spent for polymer deposition, measured at the neutral state, was ca. 40% for the vinylidene compounds **6**−**9** and 25% for the spiranic compounds **2a**−**2d** and **3**−**5**. This value indicates a dopant anion content of 0.8 and 0.5 anions per monomeric unit, respectively.

In the case of polymers derived from monomers **2a**−**2d** and **3**−**5** the CVs show a single redox process (Figure 4),[14] while in the case of materials resulting from compounds **6**−**9**, the response is a twin-peak signal (Figure 5).[25]

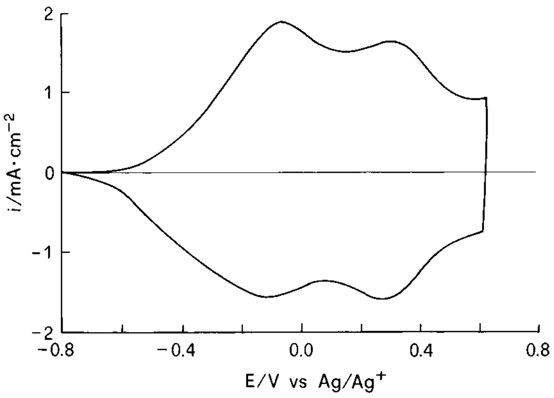

Figure 5. Anodic cyclic voltammogram for poly(**7**) in $CH_3CN + 0.1$ M Et_4NClO_4. Scan rate: 0.1 V/s. Reversible charge: 14 mC/cm^2.

The redox potentials $E°$, taken as the average of oxidation and reduction peak potentials, are given in Table 1.

$E°_{pol}$ values are ca. 0.1 V, that is, quite close to the extrapolated value for polythiophene (0.07 V vs Fc/Fc^+, corresponding to ca. 0.1 V vs Ag/Ag^+),[26] suggesting a high degree of polymerization.

Exhaustive electrolysis of the monomers produces the bulk oxidized polymers, which can then be electrochemically reduced to the neutral state. Dedoping of the materials was completed with a hydrazine treatment, followed by exhaustive washing of the resulting material with acetonitrile and drying.

The IR spectra of neutral polymers display a strong band at ca. 800 cm^{-1} due to the out-of-plane bending of inner β-CH bonds and a weak band at ca. 700−650 cm^{-1} due to the same deformation of terminal CH bonds. The ratio of their intensity allows an estimation of the degree

---

(25) Zotti, G.; Schiavon, G.; Zecchin, S.; Berlin, A.; Pagani, G. *Synth. Met.* **1994**, *66*, 149.

(26) Bauerle, P. *Adv. Mater.* **1992**, *4*, 102.

Table 1. Redox Potentials ($E°_{pol}$), Conductivities (σ), and Maximum Absorption Wavelength ($\lambda_{max.pol}$) for Polymers

monomer	$E°_{pol}$ (V)	σ (S cm^{-1})	$\lambda_{max.pol}$ (nm)
1	0.1	40	545
2a	0.0	25	560
2b	−0.05	25	580
2c	−0.05	130	590
2d	0.0	150	590
3	0.0	200	580
(−)-4	−0.04	100	580
(+)−5	−0.03	45	570
6	0.1/0.3	20	560
7	−0.1/0.3	60	640
8	−0.15/0.3	3	640
9	−0.15/0.3	1	640
10a	0.74	0.41	411
10b	0.63	0.44	419
10c	0.70	1.7	411
11	0.66	0.44	400
12a	0.15	80	545
12b	−0.11	80	580
12c	−0.10	80	580
12d	−0.06	200	600
12e	−0.03	300	590
12f	−0.05	40	550
12g	0.0	20	540
12h	0.02	30	570
12i	0.07	7	590
12l	0.12	2	640

of polymerization,[26] which turns out to be quite high [e.g., 35 for poly(**2c**) corresponding to a sequence of about 70 interconnected thiophene rings].[27]

The electronic spectral data of the neutral polymers are summarized in Table 1. The maximum absorption wavelength of poly(**2a**−**2d**), poly(**3**), and poly(**5**) films was found at ca. 575 ± 15 nm, that is, very close to the value extrapolated for an infinite polythiophene (ca. 540 nm).[14] The red shift (20−50 nm) might be due, to a large extent, to the electronic coplanarization effect of the monomers that shifts the maximum absorption from 302 nm in bithiophene to 315−320 nm in CPDT. The films of poly(**6**−**9**) display a maximum absorption wavelength at 650 ± 10 nm. Such marked red shifts are attributable to highly ordered and conjugated structures.[14]

Specific conductivities of the deposits are reported in Table 1 and lie in the 1−200 S cm^{-1} range.

(5) Quantitative Structure−Conductivity Relationship (QSPR Approach). All 26 monomers were represented by a wide set of molecular descriptors[28] summarized in the Theoretical Methods section. Using the *Genetic Algorithm-Variable Subset Selection* procedure,[29] four molecular descriptors (from about 200 calculated descriptors) were selected as those most correlated to the conductivity properties of the materials resulting from the monomers.

The experimental response σ was previously transformed into logarithmic units.

The best predictive OLS (ordinary least squares) regression model is characterized by the following regression statistics:

$$Q^2_{\mathrm{LOO}} = 78.1 \quad Q^2_{\mathrm{LMO}} = 77.1 \quad R^2 = 83.2 \quad F_{0.05;4,21} = 26.1 \quad s_y = 0.400$$

where Q^2 are the cross-validated prediction powers by the *leave-one-out* and *leave-more-out* procedures, respectively, R^2 the coefficient of determination, F the Fisher critical value, and s_y the standard error of the estimate.

The regression model descriptors and coefficients are

$$\mathrm{Log}\ \sigma = 2.405 + 0.806 \times \mathrm{nR09} - 0.060F + 7.491\eta_{3u} + 1.103K_u$$

The meanings of the model descriptors are as follows:

(i) nR09 is a structural index that represents the number of 9-atom circuits able to characterize compounds **4** and **11**, that is, acting as an indicator variable.

(ii) F is the Platt number,[30] which is a topological index related to molecular size and branching. It is defined as twice the number of connections of a molecular graph (Gordon-Scantlebury index), i.e., the number of second-order paths.

(iii) η_{3u} is a WHIM descriptor[24] that describes the compactness of the atom projections along the third principal axis, calculated from the molecular geometry.

The molecular principal axes were obtained by translation and rotation of the orthogonal (x,y,z) coordinate system to locate the origin in the geometrical center of the molecule and orient the new first axis in the direction of maximal molecular size. The projection of each atom (t_i) on each new axis and the variance of the atom distribution λ along the axis were calculated, the latter being a measure of molecular size in the considered direction. η_{3u} is a statistical index related to fourth-order central moment, representing the shape of atom distribution along the third principal axis; that is, it assumes small values where atoms are very close (high compactness) and large values where atoms are located at two opposite centers (low compactness, bimodal distribution).

(iv) K_u is a global shape WHIM descriptor[24] assuming values close to 0 for a spherical top and close to 1 for linear symmetry.

The graph reported in Figure 6 shows the regression between the experimental and the calculated conductivity values.

The molecular descriptor values for the three monomers giving the most conductive materials are found in Table 2.

Monomer **3**, for which descriptor K_u has a significantly lower value, is an outlier and the high conductivity of its polymer is underestimated in this model.

Conclusions

The most important conclusion suggested by the QSPR model is that conductivity is influenced by some different structural parameters that cannot be considered as individually operating, but as acting in a cooperative way. In fact, conductivity increases because of a concurrent lowering of molecular branching[31] and axial compactness (η_{3u}) combined with an increase in

---

(27) Furukawa, Y.; Akimoto, M.; Harada, I. *Synth. Met.* **1987**, *18*, 151.

(28) Todeschini, R.; Consonni, V. *DRAGON−Software for the Calculation of Molecular Descriptors, version 1.0 for Windows, 2000*; Talete srl: Milan, Italy. Free download available from the web page: http://www.disat.unimib.it/chm.

(29) Leardi, R.; Boggia, R.; Terrile, M. *J. Chemometrics* **1992**, *6*, 267.

(30) Todeschini, R.; Consonni, V. *Handbook of Molecular Descriptors*; Wiley-VCH: New York, in press.

(31) *Statistica Rel. 5.0 for Windows, 1995*; StatSoft, Inc.: Tulsa, OK, 1995.

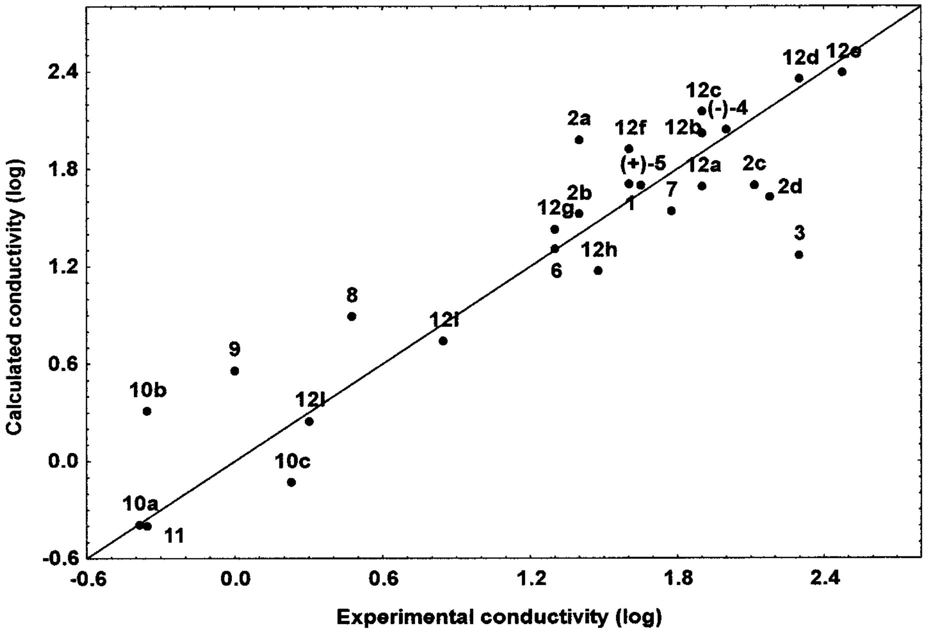

Figure 6. Regression between experimental and calculated conductivity values.

Table 2

descriptors	nR09	F	η_{3u}	K_u
min−max	0−1	38−82	0−0.366	0.182−0.792
3	0	62	0.284	0.407
12d	0	52	0.306	0.689
12e	0	56	0.328	0.792

linearity (K_u). The contribution due to the nR09 can be just considered as a specific correction factor. Concerning the compactness descriptor η_{3u} (high values are characteristic of low density in atom distribution along the third axis of the molecule), it should be noted that for almost all the monomers the third axis is approximately perpendicular to the CPDT molecular plane, with the exception of the long-chain substituted compounds (**12c**−**12e** and **12h**−**12l** monomers). According to these considerations, the most conductive materials result from monomers **12a**−**12e**, **2c**, **2d**, **3**, and **4**, where the best compromise among the parameters discussed above is realized.

Furthermore, it is known that conductivity of polyheterocycles, when not controlled by intrachain hopping, depends on the chain distance, in accordance with the VHR model.[32] Consequently, conductivity decreases progressively with the size of the interchain spacer, as shown in 3,4-disubstituted polypyrroles bearing substituents of different sizes[33] and in 3-alkyl-substituted polythiophenes (n = 1−16).[34] In our systems, the polymer chains are so long (as demonstrated by IR data) and conjugated (as demonstrated by UV−vis data) that conductivity is controlled by interchain hopping. This is the reason the typology of the substituents in position 4 of CPDT and their steric demand are crucial. Substituents extending consistently in both the emi-spaces above and below the CPDT plane negatively affect conductivity (see the polymers resulting from 4,4′-disubstituted CPDTs **12g**−**12l** and bicyclononane derivatives **8** and **9**) because they inhibit interchain hopping. Because the CPDT moiety is able to confer an unusual interchain coplanarity to the polymers, it is expected that long-shaped substituents give additional order to the chains, similar to that occurring in liquid crystals. In fact, evidence for this regular arrangement is supplied by the presence of a vibronic band at 640 nm in the IR spectra of the vinylidene monomer series.

Thus, the negative effect on conductivity due to steric encumbrance can be balanced by the positive contribution to ordering enhancement exerted by bulky substituents endowed with a specially tailored shape.

Conductivity of materials resulting from dithiafulvalenes **10a**−**10c** and **11** is probably affected by electronic factors more than by substituent size and shape.[35]

Experimental Section

Theoretical Methods. *Molecular Descriptors.* WHIM (weighted holistic invariant molecular) descriptors were used for the 3D representation of the molecules: a set formed by the 33 *nondirectional WHIM* and the 66 *directional WHIM* descriptors. WHIM descriptors are 3D-molecular indices that represent different sources of chemical information; they contain information about the whole 3D-molecular structure in terms of size, shape, symmetry, and atom distribution.[24] These indices are calculated from (x,y,z)-coordinates of a 3D structure of the molecule, from a spatial conformation of minimum energy, obtained by the software HyperChem,[23] within different weighting schemes in a straightforward manner and represent a very general approach to describe molecules in a unitary conceptual framework.

For modeling purposes, other sets of theoretical descriptors were used, in addition to the WHIM descriptors: the first one is made up of the *constitutional descriptors*, that is, the number of different kinds of atoms (for example, nH and nC are the number of hydrogens and carbons, respectively), the number

---

[32] VHR (variable range hopping) model.

[33] Ruhe, J.; Krohnke, C.; Ezquerra, T.; Kremer, F.; Wegner, G. *Ber. Bunsen-Ges. Phys. Chem.* **1987**, *91*, 885. Ruhe, J.; Ezquerra, T.; Mohammadi, M.; Enkelmann, V.; Kremer, F.; Wegner, G. *Synth. Met.* **1989**, *28*, C217.

[34] Roncali, J.; Garreau, R.; Yassar, A.; Marque, P.; Garnier, F.; Lemaire, M. *J. Phys. Chem.* **1987**, *91*, 6706.

[35] Salzner, U.; Lagowski, J. B.; Pickup, P. G.; Poirier, R. A. *J. Org. Chem.* **1999**, *64*, 7419. Salzner, U.; Kiziltepe, T. *J. Org. Chem.* **1999**, *64*, 764.

of bonds (nBO), the number of some functional groups (for example, nOH and nCO are the number of OH and CO groups, respectively), the number of rings of different sizes (nR03, ..., nR10 are the number of three-membered to ten-membered rings). Moreover, the number of atom acceptors and donors of H-bonds (nHA and nHD) are also considered. The second set is formed by the more frequently used *topological descriptors* (information and connectivity indices).[30] The molecular weight (MW) is always used, along with other empirical descriptors. The whole data set of the molecular descriptors is available upon request.

Calculations. The molecular geometries have been optimized by the *HYPERCHEM* package,[23] using the molecular mechanics method of Allinger (MM+). WHIM and the other cited molecular descriptors have been calculated from the obtained atomic coordinates using our package *DRAGON for WINDOWS/PC*.[28] The principal component analysis (PCA) was performed by the *STATISTICA* package.[31]

The selection of the best subset variables (VSS method) for modeling the given property was performed by taking a *genetic algorithm* (GA-VSS) approach. As a regression tool, the *ordinary least-squares regression* (OLS) was used as implemented in our package *MobyDigs for WINDOWS/PC*.[36]

The parameter R^2 is the multiple correlation coefficient; s_y and F are the standard error of the estimate and the Fisher critical value, respectively. All the calculations were performed using the leave-one-out procedure of cross validation, maximizing the cross-validated R^2 (Q^2_{LOO}). To avoid overestimation of the predictive capability of the models, the leave-more-out procedure (with three cross-validation groups, that is, 20% of the objects left out at each step) was also performed (Q^2_{LMO}).

For the obtained models, all variables are highly significant within a 95% confidence level.

Chemical and Electrochemical Synthesis. *General Procedures and Apparatus*. Melting points were determined on a W. Büchi apparatus and are uncorrected. ^{1}H NMR spectra were recorded on Bruker AC 300 and Varian XL 200 spectrometers with $CDCl_3$ as the solvent, unless specified otherwise. Electron-impact mass spectra were recorded on a VG 7070 EQ-HF instrument.

Electrochemical experiments were performed at 25 °C under nitrogen in three-electrode cells in CH_3CN + 0.1 M tetraethylammonium perchlorate (Et_4NClO_4). The counter electrode was platinum; the reference electrode was a silver/0.1 M silver perchlorate in acetonitrile (0.34 V vs SCE). Acetonitrile was distilled twice over P_2O_5 and once over CaH_2. The supporting electrolyte Et_4NClO_4 was previously dried under vacuum at 70 °C. The voltammetric apparatus, by AMEL (Italy), included a 551 potentiostat modulated by a 568 programmable function generator and was coupled to a 731 digital integrator. The working electrode for cyclic voltammetry was a platinum minidisk electrode (0.003 cm^2). For electronic spectroscopy a 0.8 × 2.5 cm indium tin oxide (ITO) sheet (ca. 80% transmittance, ca. 300 Ω/square resistance, from Balzers, Liechtenstein) was used. Electronic spectra were taken with a Perkin-Elmer Lambda 15 spectrometer and FTIR spectra on a Perkin-Elmer FTIR 2000 spectrometer. The apparatus and procedures used in the in situ conductivity experiments were previously described in detail.[37] The relevant working electrode was a two-band platinum electrode (0.3 × 0.01 cm for each band) with an interband spacing of 6 μm, typically polymer-coated, with the passage of 20 mC, which ensured the attainment of limiting resistance conditions. Poly(3-methylthiophene) (60 S cm^{-1}) was used as the conductivity standard.

Crystallographic data for **2d** and **8** were collected on a Siemens-P4 diffractometer using graphite monochromatized Mo $K\alpha$ radiation ($\lambda = 0.71073$ Å); the structures were solved by SIR-92[38] and refined by full-matrix least-squares based on $F_o{}^2$ (SHELXL-93).39[39]

Preparation of Spiro[*4H-cyclopenta*[*2,1-b;3,4-b′*]*dithiophene-4,1-cycloalkanes*] (***2a−d** and **3***)*: General Procedure*. A 1.6 M solution of BuLi (3.52 mmol) was slowly added to a solution of 4H-cyclopenta[2,1-b;3,4-b′]dithiophene (**1**) (3.53 mmol) in dry THF (15 mL) at −20 °C. The reaction mixture was stirred for 20 min under N_2 and then dropped into a solution of the suitable ω,ω'-dibromoalkane (3.72 mmol) in dry THF (5 mL) at −70 °C. After 30 min dry THF (10 mL) was added and a 1.6 M solution of BuLi (3.52 mmol) was dropped into the reaction mixture at −70 °C. The solution was stirred for 30 min at room temperature, then poured into water, and extracted with ether. The organic layer was separated, dried (Na_2SO_4), and concentrated in vacuo to give a residue that was column chromatographed (silica gel, hexane).

Preparation of Spiro[*2,4*]([*5,4-b;6,7-b′*]*dithieno*)*heptane* (***2a***). The first product eluted was **2a**, further purified by crystallization from pentane: yield 0.268 g (37%); mp 105 °C; ^{1}H NMR δ 7.15 (d, J = 5, 2H), 6.72 (d, J = 5, 2H), 1.75 (s, 4H); EIMS m/z 204 M$^+$. Anal. Calcd. for $C_{11}H_8S_2$: C, 64.67; H, 3.95. Found: C, 64.47; H, 4.17.

Preparation of Spiro[*3,4*]([*6,5-b;7,8-b′*]*dithieno*)*octane* (***2b***). The first product eluted was **2b** like a yellow liquid: yield 0.229 g (30%); ^{1}H NMR δ 7.20 (d, J = 5, 2H), 7.15 (d, J = 5, 2H), 2.55 (t, J = 8, 4H), 2.30 (m, 2H); EIMS m/z 218 M$^+$. Anal. Calcd. for $C_{12}H_{10}S_2$: C, 66.02; H, 4.62. Found: C, 66.27; H, 4.19.

Preparation of Spiro[*4,4*]([*2,1-b;3,4-b′*]*dithieno*)*nonane* (***2c***). The first product eluted was **2c** further purified by crystallization from pentane: yield 0.256 g (31%); mp 80 °C; ^{1}H NMR δ 7.15 (d, J = 5, 2H), 7.0 (d, J = 5, 2H), 1.9−2.1 (m, 8H); EIMS m/z 232 M$^+$. Anal. Calcd for $C_{13}H_{12}S_2$: C, 67.20; H, 5.21. Found: C, 67.44; H, 5.25.

Preparation of Spiro[*4,5*]([*2,1-b;3,4-b′*]*dithieno*)*decane* (***2d***). The first product eluted was **2d** further purified by crystallization from pentane: yield 0.394 g (45%); mp 58−60 °C; ^{1}H NMR δ 7.13 (s, 4H), 1.6−1.9 (m, 10H); EIMS m/z 246 M$^+$. Anal. Calcd. for $C_{14}H_{14}S_2$: C, 67.69; H, 5.73. Found: C, 67.90; H, 5.57.

Preparation of Dispiro[*3,1,4,1*]([*8,7-b;9,10-b′*]*dithieno*)*undecane* (***3***). The second product eluted was **3**: yield 0.088 g (26%); ^{1}H NMR δ 7.1 (s, 4H), 2.6 (s, 4H), 1.8−2.4 (m, 6H); EIMS m/z 258 M$^+$. Anal. Calcd. for $C_{15}H_{14}S_2$: C, 69.72; H, 5.46. Found: C, 69.84; H, 5.34.

Preparation of (+)-(*1S,2S*)-*Trans-bis*(*hydroxymethyl*)*cyclohexane Bis-methanesulfonate* [***(+)-14***]. Methanesulfonyl chloride (13.2 mmol) was slowly added to a solution of (−)-(1*S*,2*S*)-*trans*-bis(hydroxymethyl)cyclohexane [**(−)-13**] (5.5 mmol) in pyridine (15 mL) at −10 °C. The mixture was stirred for 3 h at −10 °C, then poured into water, and extracted with CH_2Cl_2. The organic layer was washed with 2 N HCl solution (100 mL) and then with water and dried (Na_2SO_4). The solution, concentrated in vacuo, left a residue that was further purified by crystallization from methanol to give **(+)-14**: yield 0.98 g (60%); mp 85 °C; ^{1}H NMR δ 4.20 (m, 4H), 3.02 (s, 6H), 1.95−1.05 (m, 10H); $[\alpha]^{25}_{\mathrm{D}} = +18.6°$ (c = 4, $CHCl_3$).

Preparation of (+)-*Spiro*[*4H-cyclopenta*[*2,1-b;3,4-b′*]*dithiophene-4,1′*-(*3′S,4′S*)-*dimethylcyclopentane* ***(+)-4***. A 1.6 M solution of BuLi (3.52 mmol) was slowly added to a solution of 4H-cyclopenta[2,1-b;3,4-b′]dithiophene (**1**) (3.25 mmol) in dry THF (20 mL) at −10 °C. The reaction mixture was stirred for 20 min under N_2 and then dropped into a solution of (+)-(1*S*,2*S*)-*trans*-bis(hydroxymethyl)cyclohexane bis-methanesulfonate [(+)-(3.25 mmol) in dry THF at −70 °C. After 15 min, a 1.6 M solution of BuLi (4.16 mmol) was dropped into the reaction mixture at −70 °C and then the temperature was allowed to warm to room temperature. The solution was poured into water and extracted with CH_2Cl_2. The organic layer was separated, dried (Na_2SO_4), and concentrated in vacuo to give a residue that was column chromatographed (SiO_2, hexane) and triturated with hexane to give (−)-4 yield 0.23 g (25%); mp 85 °C; ^{1}H NMR δ 7.10 (d, J = 6.4, 2H), 6.90 (d, J = 6.4,

---

(36) Todeschini, R. *MobyDigs—Software for Multilinear Regression Analysis and Variable Subset Selection by Genetic Algorithm. Rel. 2.1 for Windows, 1999*; Talete srl: Milan, Italy, 1999.

(37) Schiavon, G.; Sitran, S.; Zotti, G. *Synth. Met.* **1989**, *32*, 209.

(38) Altomare, A.; Cascarano, G.; Giacovazzo, G.; Guagliardi, A.; Burla, M. C.; Polidori, G.; Camalli, M. *J. Appl. Crystallogr.* **1994**, *27*, 435.

(39) Sheldrick, G. M. *SHELXL-93*; University of Göttingen, Germany, 1993.

2H), 2.00−1.15 (m, 14H); $[\alpha]^{25}_{D} = -63.6°$, $[\alpha]^{25}_{578} = -66.7°$, $[\alpha]^{25}_{546} = -76.3°$ ($c = 1$, MeOH); UV (CH_2Cl_2): 318, 250, 224 nm. Anal. Calcd for $C_{17}H_{18}S_2$: C, 71.36; H, 6.31. Found: C, 71.22; H, 6.05.

Preparation of (−)-(2*R*,3*R*)-*Dimethyl-1,4-butanediol Bismethanesulfonate* [**(−)-16**]. **(−)-16** was prepared according to the procedure described above for **(+)-14**, starting from (+)-(2*R*,3*R*)-dimethyl-1,4-butanediol [**(+)-15**] (5.5 mmol); yield 1.026 g (68%); mp 65−68 °C; ^{1}H NMR δ 4.10 (d, $J = 6.1$, 4H), 3.00 (s, 2H), 2.10 (m, 2H), 0.95 (d, $J = 7.6$, 6H); $[\alpha]^{25}_{D} = -1.3°$ ($c = 5$, CH_2Cl_2).

Preparation of (+)-*Spiro*[*4H-cyclopenta*[*2,1-b*;*3,4-b′*]*dithiophene-4,1′*-(*3′S,4′S*)-*dimethylcyclopentane* [**(+)-5**]. The title compound was prepared according to the procedure described above for **(−)-4** starting from (−)-(2*R*,3*R*)-dimethyl-1,4-butanediol dimethanesulfonate [**(−)-16**] (3.25 mmol): yield 0.345 g (41%); mp 105−107 °C; ^{1}H NMR δ 7.10 (d, $J = 6.4$, 2H), 6.90 (d, $J = 6.4$, 2H), 2.15 (dd, $J_1 = 11.9$, $J_2 = 6.0$, 2H), 1.87 (m, 2H), 1.78 (m, 2H), 1.12 (d, $J = 5.5$, 6H); $[\alpha]^{25}_{D} = +46.8°$, $[\alpha]^{25}_{578} = +49.2°$, $[\alpha]^{25}_{546} = +57.5°$ ($c = 4$, CH_2Cl_2); UV (CH_2Cl_2) 318, 250, 222 nm. Anal. Calcd for $C_{15}H_{16}S_2$: C, 69.27; H, 6.17. Found: C, 70.01; H, 6.01.

Preparation of Isopropylidencyclopenta[*2,1-b*;*3,4-b′*]*dithiophene* (**6**). A 1.6 M solution of BuLi (3.52 mmol) was added to a solution of 4H-cyclopenta[2,1-b;3,4-b′]dithiophene (**1**) (2.30 mmol) in dry THF (15 mL) at room temperature. After 15 min, a solution of acetone (2.4 mmol) in THF (5 mL) was added. The reaction mixture was stirred for 2 h under N_2 at room temperature, then poured into water, and extracted with ether. The organic layer was separated, dried (Na_2SO_4), and concentrated under reduced pressure to give a residue. Chromatography (SiO_2, hexane) provided pure **6**: yield 0.201 g (40%); mp 80−83 °C; ^{1}H NMR δ 7.3 (d, $J = 5$, 2H), 7.1 (d, $J = 5$, 2H), 2.4 (s, 6H); EIMS *m*/*z* 218 M^+. Anal. Calcd for $C_{12}H_{10}S_2$: C, 66.02; H, 4.62. Found: C, 66.15; H, 4.58.

Preparation of Cyclohexylidencyclopenta[*2,1-b*;*3,4-b′*]*dithiophene* (**7**). The title compound was prepared according to the procedure described above starting from cyclohexanone (2.4 mmol). The residue was treated with isopropyl ether to give **7**: yield 0.23 g (33%); mp 114−119 °C; ^{1}H NMR δ 7.35 (d, $J = 5$, 2H), 7.05 (d, $J = 5$, 2H), 3.00−1.70 (m, 10H); EIMS *m*/*z* 258 M^+. Anal. Calcd. for $C_{15}H_{14}S_2$: C, 69.80; H, 5.44, Found: C, 69.97; H, 5.66.

Preparation of 9-(*4H−Cyclopenta*[*2,1-b*;*3,4-b′*]*dithiophenyl*)-*9-bicyclo*[*3,3,1*]*nonanol* (**17**). A 1.6 M solution of BuLi (2.80 mmol) was dropped into a solution of 4H-cyclopenta[2,1-b;3,4-b′]dithiophene (**1**) (2.80 mmol) in dry THF (15 mL) at room temperature under N_2. After 15 min, a solution of the bicyclo-[3.3.1]nonan-9-one (2.86 mmol) in THF (5 mL) was added. The reaction mixture was stirred for 1 h under N_2 at room temperature, then poured into water, and extracted with CH_2Cl_2. The organic layer was separated, dried (Na_2SO_4), and concentrated in vacuo. The crude reaction product was treated with isopropyl ether to give 9-(4H-cyclopenta[2,1-b;3,4-b′]-dithiophenyl)-9-bicyclo[3,3,1]nonanol (**17**): yield 0.51 g (57%); mp 210−215 °C; ^{1}H NMR δ 7.20 (d, $J = 4.7$, 2H), 7.05 (d, $J = 4.7$, 2H), 4.40 (s, 1H), 1.4−2.4 (m, 14H).

Preparation of 4-(*9-bicyclo*[*3,3,1*]*nonanyliden*)*cyclopenta*[*2,1-b*;*3,4-b′*]*dithiophene* (**8**). A mixture of 9-(4H-cyclopenta[2,1-b;3,4-b′]dithiophenyl)-9-bicyclo[3,3,1]nonanol (**17**) (1.60 mmol) and PTSA (0.58 mmol) was dissolved in toluene, refluxed for 1 h, then poured into water, and exhaustively extracted with ether. The organic layer was dried (Na_2SO_4) and evaporated to dryness to give a residue that was column chromatographed (SiO_2, hexane), yielding 4-(9-bicyclo[3,3,1]nonayliden)cyclopenta-[2,1-b;3,4-b′]dithiophene (**8**): yield 0.406 g (85%); mp 203−205 °C; ^{1}H NMR ($CDCl_3$) δ 7.25 (d, $J = 4.7$, 2H), 7.10 (d, $J = 4.7$, 2H), 3.65 (m, 2H), 1.80−2.20 (m, 12H); EIMS *m*/*z* 298 M^+. Anal. Calcd for $C_{18}H_{19}S_2$: C, 72.28; H, 6.37. Found: C, 71.88; H, 6.10.

Preparation of 2-(*4H-Cyclopenta*[*2,1-b*;*3,4-b′*]*dithiophenyl*)-*2-adamantanol* (**18**). The title compound was prepared according to the procedure described for **17**, starting from 2-adamantanone (2.86 mmol): yield 0.54 g (64%); mp 187−190 °C; ^{1}H NMR δ 7.0 (d, $J = 4.8$, 2H), 7.2 (d, $J = 4.8$, 2H), 4.40 (s, 1H), 1.4−2.5 (m, 16H).

Preparation of 4-(*2-Adamantylidene*)*cyclopenta*[*2,1-b*;*3,4-b′*]-*dithiophene* (**9**). The above compound was prepared according to the procedure described for **8** starting from **18**: yield 0.47 g (88%); mp 188−191 °C; ^{1}H NMR δ 7.25 (d, $J = 4.8$, 2H), 7.10 (d, $J = 4.8$, 2H), 3.60 (m, 2H), 1.80−2.20 (m, 12H); EIMS *m*/*z* 310 M^+. Anal. Calcd for $C_{19}H_{18}S_2$: C, 73.58; H, 5.82. Found: C, 73.97; H, 6.01.

Crystallographic Data of ***2d***. The data for **2d** are as follows: $C_{14}H_{14}S_2$, $M_r = 246.37$, monoclinic, $P2_1/n$, gold-yellow, $0.40 \times 0.40 \times 0.22$ mm^3, $a = 15.7886(11)$ Å, $b = 10.0214(7)$ Å, $c = 16.1420(12)$ Å, $\beta = 101.046(6)°$, $Z = 8$, $d_{calc} = 1.333$ g cm^{-3}, μ(Mo Kα) = 0.402 mm^{-1}, temperature 293(2) K, data collection range $2.42° < \theta < 25.00°$, $\theta/2\theta$ scan mode, 4491 collected reflections, 4325 independent, 3403 with $I > 2\sigma(I)$, no absorption correction, anisotropic heavy atoms, isotropic hydrogen atoms, 402 parameters refined, final disagreement factors based on 4325 (3403) F_o^2: $R = 0.0542$ (0.0380), wR = 0.1002 (0.0896), and GOF = 1.022. The asymmetric unit holds two independent molecules; their difference is very small: equivalent bond distances are all within 3 standard uncertainties and only 5 bond angles exceed this limit, while the maximum difference on torsion angles is <3°. The molecules shows only small deviations from C_s symmetry: the continuous symmetry measure[40] calculated by *SYMMOL*[41] is only 0.04 and 0.06 for molecule A and B, respectively. The small deviation from C_s symmetry of the insulated molecule agrees with the very weak intermolecular interactions.

Crystallographic data of ***8***. The data for **8** are as follows: $C_{18}H_{18}S_2$, $M_r = 298.44$, tetragonal, $P4_32_12$, gold-yellow, $0.40 \times 0.20 \times 0.16$ mm^3, $a = 10.6898(9)$ Å, $c = 12.9090(13)$ Å, $Z = 4$, $d_{calc} = 1.344$ g cm^{-3}, μ(Mo Kα) = 0.348 mm^{-1}, temperature 293(2) K, data collection range $2.47° < \theta < 25.00$ °, $\theta/2\theta$ scan mode, 1638 collected reflections, 1302 independent, 998 with $I > 2\sigma(I)$, no absorption correction, anisotropic heavy atoms, isotropic hydrogen atoms, 129 parameters refined, and final disagreement factors based on 1302 (998) F_o^2: $R = 0.0676$ (0.0422), wR = 0.0976 (0.0853), and GOF = 1.061.

The molecule lies on a crystallographic C_2 axis; the insulated molecule probably shows the same molecular symmetry; the crystal packing shows very weak interactions and may with great difficulty be responsible for the loss of molecular C_{2v} symmetry. In fact, C_{2v} symmetry is on a saddle point with respect to the conformational energy because of the strain due to the short intramolecular distance H3...H13; the minimum energy is reached, enlarging the angles C4−C11−C12 and C11−C12−C13 from the ideal sp^2 angle to 127.9(2)° and 125.0-(2)°, respectively, and with a torsion of 10.1(2)° around the double bond C11−C12.

Supporting Information Available: Tables of final coordinates and of atomic displacement parameters for **2d** and **8** (CIF). This material is available free of charge via the Internet at http://pubs.acs.org.

CM0009118

---

(40) Zabrodsky, H.; Peleg, S.; Avnir, D. *J. Am. Chem. Soc.* **1993**, *114*, 8278.

(41) Pilati, T.; Forni, A. *J. Appl. Crystallogr.* **1998**, *31*, 503.